Enamine-based cross-linkable hole-transporting materials for perovskite solar cells

*Deimantė Vaitukaitytė, Amran Al-Ashouri, Marytė Daškevičienė, Egidijus Kamarauskas, Jonas Nekrasovas, Vygintas Jankauskas, Artiom Magomedov, Steve Albrecht, Vytautas Getautis**

D. Vaitukaitytė, Dr. M. Daškevičienė, Dr. A. Magomedov, Prof. V. Getautis
Department of Organic Chemistry, Kaunas University of Technology, Radvilenu pl. 19, Kaunas LT-50254, Lithuania.
E-mail: vytautas.getautis@ktu.lt

A. Al-Ashouri, Prof. S. Albrecht
Young Investigator Group Perovskite Tandem Solar Cells, Helmholtz-Zentrum Berlin, Kekuléstraße 5, 12489 Berlin, Germany.

Dr. E. Kamarauskas, J. Nekrasovas, Dr. V. Jankauskas
Institute of Chemical Physics, Vilnius University, Sauletekio al. 3, Vilnius 10257, Lithuania

Prof. S. Albrecht
Faculty of Electrical Engineering and Computer Science, Technical University Berlin, Marchstraße 23, 10587 Berlin, Germany

Keywords: enamines, cross-linking, hole-transporting materials, perovskite solar cells.

The development of the simple synthesis schemes of the organic semiconductors can have an important contribution to the advancement of the related technologies. In particular, one of the fields, where the high price of the hole-transporting material may become an obstacle towards successful commercialization, is perovskite solar cells. In this work, we have synthesized enamine-based materials that are capable to undergo cross-linking due to the presence of the two vinyl groups. It was shown that new compounds can be thermally polymerized, making the

films resistant to organic solvents. This can allow to use a wet-coating process for the deposition of the perovskite absorber film, without the need for orthogonal solvents. Cross-linked films were used in perovskite solar cells, and, upon optimization of the film thickness, the highest power conversion efficiency of 18.1% was demonstrated.

1. Introduction

Perovskite solar cells (PSCs) have recently demonstrated efficiencies comparable to that of the best Si-based technologies.[1] Among other things, further advancement of PSCs depends on the development of novel materials that can serve as efficient hole transporters.[2] However, the choice of the organic hole-transporting materials (HTMs), able to deliver competitive performance, is still limited. Therefore, it is important to search for the new promising organic materials.

As an additional constrain, to keep the transition from lab to fab as fast as possible, it is advantageous to maintain the simplicity of the organic materials as one of the highest priorities. It is thus necessary to use simple and short synthesis pathways since it was recently shown that multi-step schemes lead to extremely high materials costs.[3] In addition, it is better to avoid the use of metal-catalyzed reactions, as metal traces are known to have detrimental effects on the performance of optoelectronic devices,[4] and therefore additional purification processes (e.g. sublimation[5]) are required, which further increases the price of the final material. In this context, condensational chemistry is giving possibilities to increase the π-conjugated system of the molecules in a simple way, with water as the only by-product. The simplicity of the synthesis and purification can promote the wider application of such materials.

One of the semiconducting material classes that fulfill the above-mentioned requirements is enamines. Typically, they are synthesized from aromatic amine and aromatic ketone/aldehyde. First studies of their charge-transporting abilities were reported back in the

1980s,[6–8] and since then they were successfully incorporated in electrophotographic devices[9] and OLEDs,[10] and recently were reported to show good performance in PSCs.[11,12,13]

Depending on the order of the layers in the final device, PSCs are commonly divided into two large groups. Currently, the highest certified efficiency, published in peer-reviewed journals (22.7%), was achieved in a so-called "regular", or n-i-p configuration, where HTM is deposited on top of the perovskite absorber layer.[14] As an alternative, in recent years, also p-i-n (or "inverted") configuration of PSCs was established, with efficiencies getting close to that of the best PSCs (highest published certified value of 22.3%),[15] and in addition, having advantages in tandem applications.[16,17] In the case of p-i-n devices, solution-processing of the perovskite absorber layer adds additional constraints on the choice of HTMs, as it usually should withstand a mixture of polar DMF:DMSO solvents. The perovskite precursor solution has significantly lower ability to dissolve organic HTMs (**Table S1**), however, it is enough to reduce the scope of the applicable materials. Therefore, so far the most popular choice of organic HTMs for such devices are polymers, such as PTAA[18] and PEDOT:PSS.[19] Recently, different small-molecule HTMs for p-i-n have been reported, such as MPA‑BTTI,[20] BTF4,[21] BDPSO[22] etc., however, their number is still rather limited due to the above mentioned restriction. Therefore, as an alternative, several strategies were reported, e.g. change of the perovskite precursor solvent,[23] use of self-assembled monolayers,[24] or use of soluble precursors that are subsequently transformed into insoluble films.[25] In addition, recently cross-linkable HTMs were introduced into inverted devices, resulting in relatively high performances.[26] However, it was achieved using palladium-catalyzed reactions.

In this work, enamine-based cross-linkable HTMs, containing two vinyl groups, were synthesized and investigated. We show that new materials can undergo thermal polymerization, forming solvent-resistant films. The polymerization process has a negligible effect on the electrical properties of the materials. As a proof of concept, PSCs of p-i-n

configuration were constructed, and devices with polymerized **V1187** showed a promising PCE of 18.14%, showing a great potential of the presented class of dopant-free organic HTMs.

2. Results and discussions

For the target materials to undergo *in situ* cross-linking, it is required to incorporate at least two groups that can undergo polymerization into the structure of the final compounds. To do so, commercially available fluorene amines were chosen as starting compounds, and following a simple two-step reaction scheme (**Scheme S1**, **Scheme S2**), two final compounds **V1162** and **V1187** were obtained (**Figure 1**). Detailed synthesis procedures are reported in supporting information. In brief, during the first step, starting amines were condensed with 2,2-bis(4-methoxyphenyl)acetaldehyde, following a previously published procedure,[11] and intermediate compounds **1** and **2** were isolated via crystallization in 47% and 94% yields respectively. During the second step, intermediate compounds were alkylated by 4-vinylbenzylchloride, to obtain final compounds **V1162** and **V1187** with good yields (74% and 59% respectively). Structures of the synthesized compounds were confirmed by means of NMR and elemental analysis.

Following a previously published procedure,[3] the costs of the materials used for the synthesis were evaluated (detailed calculations can be found in supporting information). The calculated price of the materials is 13.56 €/g and 16.34 €/g for **V1162** and **V1187**, respectively, which is somewhat higher than that of the lowest reported costs of organic HTMs (e.g. V950 ~6 €/g,[11] EDOT-Amide-TPA ~5$/g[27]), however, is significantly lower than that of the most popular HTM Spiro-OMeTAD (93$/g[28]).

In order to evaluate the optical properties of the synthesized compounds, UV/vis, and photoluminescence (PL) spectra were recorded from the solutions, and the results are presented in **Figure S2**. The enamine **V1162** has an absorption maximum (λ_{max}) in the UV range at 370 nm, with only negligible absorption in the visible range of electromagnetic

radiation. The compound **V1187** with its additional enamine branch has a bathochromically shifted λ_{max} of 406 nm due to the larger π-conjugated electrons system, giving a slightly stronger light absorption in the visible range. This might reduce the performance of the p-i-n PSC, where the light first passes through the HTM layer, however, if the film thickness is small, the drop in J_{sc} should not be significant. In addition, from the PL spectra, it can be seen that emission of the **V1187** is slightly red-shifted by 7 nm, in comparison to that of **V1162**, which is consistent with the increased π-conjugated electron system.

For the evaluation of the thermal stability of the materials and their ability to undergo a cross-linking process, thermal properties were studied by means of differential scanning calorimetry (DSC) and thermogravimetric analysis (TGA). For the **V1162**, during the first DSC heating cycle (**Figure 2**), the glass transition process was detected at 100 °C, followed by a melting process at 228 °C, showing that the material after purification has a mixture of amorphous and crystalline states. Directly after melting, an exothermic process was detected at 231 °C, suggesting that thermal polymerization occurs at this temperature. During the second heating cycle, no phase transitions were observed, confirming a formation of the cross-linked polymer. For **V1187**, with higher molecular weight, a slightly higher T_g of 136 °C was detected and no melting process was observed, suggesting that **V1187** was isolated as an amorphous material. The cross-linking process started at ~190 °C, with a peak at around 239 °C. Again, during the second heating cycle, no phase transitions were detected. In addition, both compounds showed excellent thermal stability, with a T_d of 396 °C for **V1162** and 393 °C for **V1187**, as can be seen from TGA analysis (**Figure S1**).

To evaluate the cross-linking ability of the thin films of the new HTMs, they were analyzed by evaluating the amount of washed material from the spin-coated film, by means of UV/vis spectroscopy (detailed cross-linking procedure can be found in the supporting information). The results are presented in **Figure 3**. After heating the HTM films at 231 °C, already after 15 minutes, the majority of the monomer was cross-linked into an insoluble polymer. Very

similar behavior was observed for both **V1162** and **V1187** materials, and the process of the cross-linking was complete roughly after 45 minutes of heating. The cross-linked films have shown to be resistant to the DMF:DMSO (4:1) solvents, as after exposure to them the UV/vis absorption spectra of the films remained almost the same (**Figure S4**, **Figure S5**). As an additional indication of the conversion of the vinyl groups, FT-IR spectra were recorded (**Figure S6**). After annealing, the characteristic peaks of the vinyl groups at the 988-991 cm^{-1} and 904-908 cm^{-1} has disappeared, which was previously reported to show a complete cross-linking.[29,30] Next, to study the electrical properties of the synthesized HTMs, hole drift mobility was measured with the xerographic time-of-flight (XTOF) technique (**Figure 4**). **V1187** showed very good charge transporting properties, reaching 10^{-2} cm^2/Vs at strong electrical fields. The simpler compound **V1162** showed slightly lower hole drift mobilities, yet still comparable to that of popular HTMs for PSCs. As the cross-linking process is not affecting the chromophoric system of the HTMs, it had only a minor influence on the hole drift mobility. For **V1187** the value stayed virtually the same, while for **V1162** after cross-linking mobility became roughly two times lower (Figure 4). In addition to charge transporting properties, ionization potentials were measured through photoelectron spectroscopy in air (PESA). The values were 5.11 eV and 5.26 eV for **V1187** and **V1162** respectively. Such values are consistent with the values reported for other HTMs used in PSCs.

To evaluate the performance of the materials acting as hole-selective layers in PSCs, devices with the p-i-n architecture were fabricated and characterized. As an absorber material, triple-cation perovskite was used,[31] with a nominal precursor solution composition of $Cs_{0.05}(FA_{0.83}MA_{0.17})_{0.95}Pb(I_{0.83}Br_{0.17})_3$ (see **Figure S8** for the top-view and cross-section SEM images of the best device). The films of the organic HTMs were prepared by spin-coating from toluene, and afterward, they were annealed in a nitrogen atmosphere at 230 °C for 45 minutes for the cross-linking, as was determined previously. The J/V curves are reported in

reverse (from open to short circuit) direction, as the devices have shown only a minor hysteresis (**Figure S11**). A detailed description of the fabrication and characterization of the devices can be found in SI.

First, to check the influence of the cross-linking on the performance of the devices, we have compared thermally cross-linked HTM films with that of the neat films. Via profilometry we measured no significant surface morphology differences after the cross-linking process (**Figure S3**). As can be seen from **Figure 5** and **Table 1**, for both **V1162** and **V1187** devices with the monomer films showed low open-circuit voltages (V_{oc}) (0.85 V for **V1162**, and 0.89 V for **V1187** on average). It can be attributed to the formation of direct contact between perovskite and ITO, due to the damage of the HTM film during solution-processing of the perovskite film. This in turn is lead to increased interfacial recombination, which reduces V_{oc}.[32,33] In contrast, for both materials after thermal polymerization, V_{oc} was significantly improved up to 1.04 V on average. Quite a different trend can be observed for the *FF*, where higher values were obtained for neat films (75.8 % for **V1162**, and 79.3 % for **V1187** on average), which can be attributed to the high conductivity of the ITO, and as a consequence fast transport of charges. This result is supporting the previous statement that after cross-linking the HTM films have improved resistance against solvents.

V1187 allowed for higher fill factors (*FF*) than **V1162** (**Figure 5**), and as a consequence, the highest PCE of 16.8%. As the films are used without oxidizing dopants, such improvement can be attributed to the higher values of the hole drift mobilities,[34] and as a result better transport of the charges through the film.

To further optimize the HTM film, the concentration of the **V1187** starting solution was varied from 2mg/ml down to 0.5mg/ml in toluene. As expected, the lower concentration led to the improved *FF*, however at the cost of reduced V_{oc} (**Figure 6**, **Table 2**). Steady-state PL measurements of the perovskite films on this concentration series revealed a reduced intensity of the emission with lower concentration (**Figure S9**). As the extraction abilities of the

material should be independent of the concentration, such behavior can be attributed to insufficient coverage of the ITO substrate and increased direct contact between perovskite and ITO.[35] As a result of increased interface recombination, the reduction in V_{oc} is observed. Overall, and optimized PCE of 18.1% for the cross-linked films prepared from the 1.5 mg/ml solutions were achieved.

Conclusion

In conclusion, in this work, two new enamine-based hole-transporting materials were synthesized and investigated. Due to the presence of two vinyl groups, materials **V1162** and **V1187** are able to undergo thermal cross-linking during the heating at 230 °C. After ~45 min the deposited films became resistant towards organic solvents. It was further shown that polymerization leads only to minor changes in hole drift mobilities, therefore the materials are suitable for the application in p-i-n perovskite solar cells. As a result, devices with the thermally cross-linked films have shown advantageous performance, mainly due to the higher open-circuit voltage. After further optimization of the concentration of the **V1187** solution, perovskite solar cells have shown over 18% power conversion efficiency, demonstrating a great promise of the presented strategy.

Supporting Information

Supporting Information is available from the Wiley Online Library or from the author.

Acknowledgements

This research has mainly received funding from the Research Council of Lithuania (grant No. MIP-19-14). A.A.A. and S.A. acknowledge funding from the Federal Ministry of Education and Research (BMBF) for funding of the Young Investigator Group Perovskite Tandem Solar Cells within the program “Materialforschung für die Energiewende” (grant no. 03SF0540), the Helmholtz Association within the HySPRINT Innovation Lab project, and the HyPerCells Graduate School.

Received: ((will be filled in by the editorial staff))
Revised: ((will be filled in by the editorial staff))
Published online: ((will be filled in by the editorial staff))

References

[1] National Renewable Energy Laboratory (NREL), "Best Research-Cell Efficiency Chart," **2019**.

[2] A. K. Jena, A. Kulkarni, T. Miyasaka, *Chem. Rev.* **2019**, *119*, 3036.

[3] T. P. Osedach, T. L. Andrew, V. Bulović, *Energy Environ. Sci.* **2013**, *6*, 711.

[4] C. Bracher, H. Yi, N. W. Scarratt, R. Masters, A. J. Pearson, C. Rodenburg, A. Iraqi, D. G. Lidzey, *Org. Electron.* **2015**, *27*, 266.

[5] K. Rakstys, M. Saliba, P. Gao, P. Gratia, E. Kamarauskas, S. Paek, V. Jankauskas, M. K. Nazeeruddin, *Angew. Chemie - Int. Ed.* **2016**, *55*, 7464.

[6] S. L. Rice, R. D. Balanson, R. Wingard, *J. Imaging Sci.* **1985**, *29*, 7.

[7] J. A. Sinicropi, J. R. Cowdery-Corvan, E. H. Magin, P. M. Borsenberger, *Chem. Phys.* **1997**, *218*, 331.

[8] Y. Morishita, Y. Sugimoto, H. Ishikawa, S. Hayashida, T. Okamoto, N. Hayashi, *Synth. Met.* **1991**, *41*, 1231.

[9] A. Matoliukstyte, E. Burbulis, J. V. Grazulevicius, V. Gaidelis, V. Jankauskas, *Synth. Met.* **2008**, *158*, 462.

[10] R. Paspirgelyte, R. Zostautiene, G. Buika, J. V. Grazulevicius, S. Grigalevicius, V. Jankauskas, C. C. Chen, Y. C. Chung, W. B. Wang, J. H. Jou, *Synth. Met.* **2010**, *160*, 162.

[11] M. Daskeviciene, S. Paek, Z. Wang, T. Malinauskas, G. Jokubauskaite, K. Rakstys, K. T. Cho, A. Magomedov, V. Jankauskas, S. Ahmad, H. J. Snaith, V. Getautis, M. K. Nazeeruddin, *Nano Energy* **2017**, *32*, 551.

[12] D. Vaitukaityte, Z. Wang, T. Malinauskas, A. Magomedov, G. Bubniene, V. Jankauskas, V. Getautis, H. J. Snaith, *Adv. Mater.* **2018**, 1803735.

[13] M. Steponaitis, M.-G. La-Placa, İ. C. Kaya, G. Bubniene, V. Jankauskas, M. Daskeviciene, M. Sessolo, T. Malinauskas, H. J. Bolink, V. Getautis, *Sustain. Energy*

Fuels **2020**, *4*, 5017.

[14] E. H. Jung, N. J. Jeon, E. Y. Park, C. S. Moon, T. J. Shin, T. Y. Yang, J. H. Noh, J. Seo, *Nature* **2019**, *567*, 511.

[15] X. Zheng, Y. Hou, C. Bao, J. Yin, F. Yuan, Z. Huang, K. Song, J. Liu, J. Troughton, N. Gasparini, C. Zhou, Y. Lin, D. J. Xue, B. Chen, A. K. Johnston, N. Wei, M. N. Hedhili, M. Wei, A. Y. Alsalloum, P. Maity, B. Turedi, C. Yang, D. Baran, T. D. Anthopoulos, Y. Han, Z. H. Lu, O. F. Mohammed, F. Gao, E. H. Sargent, O. M. Bakr, *Nat. Energy* **2020**, *5*, 131.

[16] J. Xu, C. C. Boyd, Z. J. Yu, A. F. Palmstrom, D. J. Witter, B. W. Larson, R. M. France, J. Werner, S. P. Harvey, E. J. Wolf, W. Weigand, S. Manzoor, M. F. A. M. Van Hest, J. J. Berry, J. M. Luther, Z. C. Holman, M. D. McGehee, *Science* **2020**, *367*, 1097.

[17] Y. Hou, E. Aydin, M. De Bastiani, C. Xiao, F. H. Isikgor, D. J. Xue, B. Chen, H. Chen, B. Bahrami, A. H. Chowdhury, A. Johnston, S. W. Baek, Z. Huang, M. Wei, Y. Dong, J. Troughton, R. Jalmood, A. J. Mirabelli, T. G. Allen, E. Van Kerschaver, M. I. Saidaminov, D. Baran, Q. Qiao, K. Zhu, S. De Wolf, E. H. Sargent, *Science* **2020**, *367*, 1135.

[18] M. Stolterfoht, C. M. Wolff, J. A. Márquez, S. Zhang, C. J. Hages, D. Rothhardt, S. Albrecht, P. L. Burn, P. Meredith, T. Unold, D. Neher, *Nat. Energy* **2018**, *3*, 847.

[19] W. Nie, H. Tsai, R. Asadpour, J. C. Blancon, A. J. Neukirch, G. Gupta, J. J. Crochet, M. Chhowalla, S. Tretiak, M. A. Alam, H. L. Wang, A. D. Mohite, *Science* **2015**, *347*, 522.

[20] Y. Wang, W. Chen, L. Wang, B. Tu, T. Chen, B. Liu, K. Yang, C. W. Koh, X. Zhang, H. Sun, G. Chen, X. Feng, H. Y. Woo, A. B. Djurišić, Z. He, X. Guo, *Adv. Mater.* **2019**, *31*, 1902781.

[21] X. Sun, Q. Xue, Z. Zhu, Q. Xiao, K. Jiang, H. L. Yip, H. Yan, Z. Li, *Chem. Sci.* **2018**, *9*, 2698.

[22] R. Shang, Z. Zhou, H. Nishioka, H. Halim, S. Furukawa, I. Takei, N. Ninomiya, E. Nakamura, *J. Am. Chem. Soc.* **2018**, *140*, 5018.

[23] C. Wang, J. Hu, C. Li, S. Qiu, X. Liu, L. Zeng, C. Liu, Y. Mai, F. Guo, *Sol. RRL* **2019**, 1900389.

[24] A. Magomedov, A. Al-Ashouri, E. Kasparavičius, S. Strazdaite, G. Niaura, M. Jošt, T. Malinauskas, S. Albrecht, V. Getautis, *Adv. Energy Mater.* **2018**, *8*, 1801892.

[25] K. Rakstys, M. Stephen, J. Saghaei, H. Jin, M. Gao, G. Zhang, K. Hutchinson, A. Chesman, P. L. Burn, I. Gentle, P. E. Shaw, *ACS Appl. Energy Mater.* **2020**, *3*, 889.

[26] Y. Zhang, C. Kou, J. Zhang, Y. Liu, W. Li, Z. Bo, M. Shao, *J. Mater. Chem. A* **2019**, *7*, 5522.

[27] M. L. Petrus, K. Schutt, M. T. Sirtl, E. M. Hutter, A. C. Closs, J. M. Ball, J. C. Bijleveld, A. Petrozza, T. Bein, T. J. Dingemans, T. J. Savenije, H. Snaith, P. Docampo, *Adv. Energy Mater.* **2018**, *8*, 1801605.

[28] M. L. Petrus, T. Bein, T. J. Dingemans, P. Docampo, *J. Mater. Chem. A* **2015**, *3*, 12159.

[29] Z. Li, Z. Zhu, C.-C. Chueh, J. Luo, A. K.-Y. Jen, *Adv. Energy Mater.* **2016**, *6*, 1601165.

[30] S. Abraham, G. P. T. Ganesh, S. Varughese, B. Deb, J. Joseph, *ACS Appl. Mater. Interfaces* **2015**, *7*, 25424.

[31] M. Saliba, T. Matsui, J.-Y. Seo, K. Domanski, J.-P. Correa-Baena, M. K. Nazeeruddin, S. M. Zakeeruddin, W. Tress, A. Abate, A. Hagfeldt, M. Grätzel, **2016**, *9*, 1989.

[32] M. Stolterfoht, P. Caprioglio, C. M. Wolff, J. A. Márquez, J. Nordmann, S. Zhang, D. Rothhardt, U. Hörmann, Y. Amir, A. Redinger, L. Kegelmann, F. Zu, S. Albrecht, N. Koch, T. Kirchartz, M. Saliba, T. Unold, D. Neher, *Energy Environ. Sci.* **2019**, *12*, 2778.

[33] J. P. Correa-Baena, W. Tress, K. Domanski, E. H. Anaraki, S. H. Turren-Cruz, B.

Roose, P. P. Boix, M. Grätzel, M. Saliba, A. Abate, A. Hagfeldt, *Energy Environ. Sci.* **2017**, *10*, 1207.

[34] W. Zhou, Z. Wen, P. Gao, *Adv. Energy Mater.* **2018**, *8*, 1702512.

[35] E. M. Hutter, T. Kirchartz, B. Ehrler, D. Cahen, E. Von Hauff, *Appl. Phys. Lett.* **2020**, *116*, 100501.

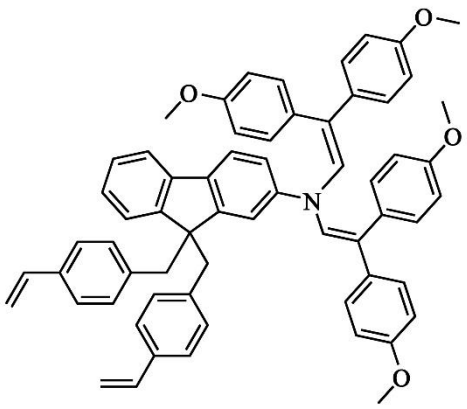

V1162

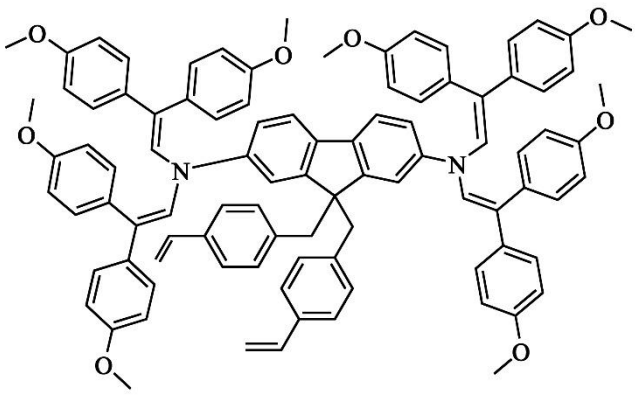

V1187

Figure 1. Molecular structures of the synthesized cross-linkable HTMs **V1162** and **V1187**.

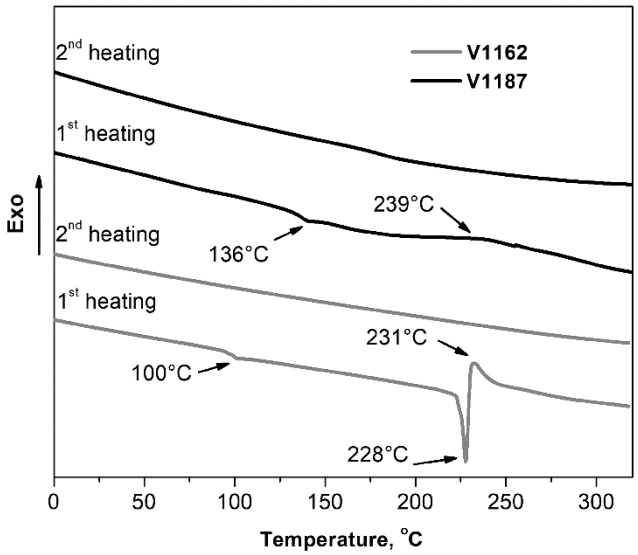

Figure 2. First and second scan heating curves of **V1162** and **V1187** (heating rate 10 °C min^{-1}, the y-axis is showing a heat flux).

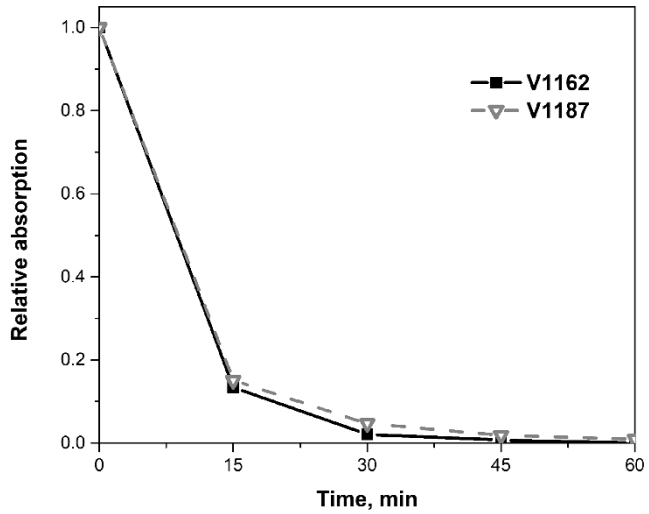

Figure 3. Cross-linking experiment of the **V1162** and **V1187** films. The absorption (at 370 nm for **V1162**, and at 406 nm for **V1187**) of the solutions, prepared by dipping spin-coated HTM films into THF after heating at 231 °C for the respective times, relative to the absorption of the solution, prepared by dipping of the non-cross-linked film.

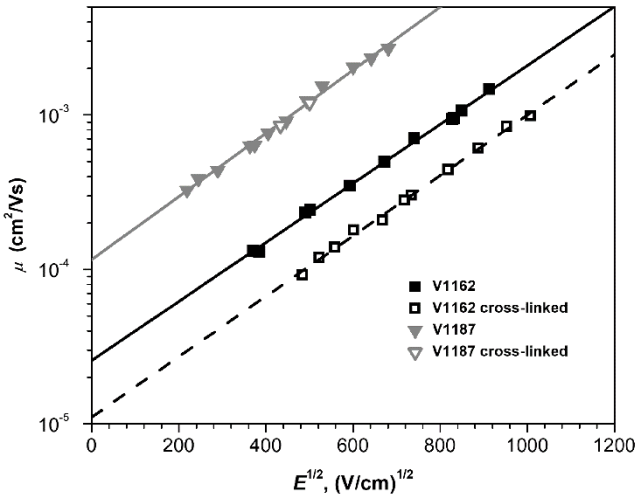

Figure 4. Electric-field dependencies of the hole drift mobilities in films of **V1162** and **V1187** before and after thermal cross-linking.

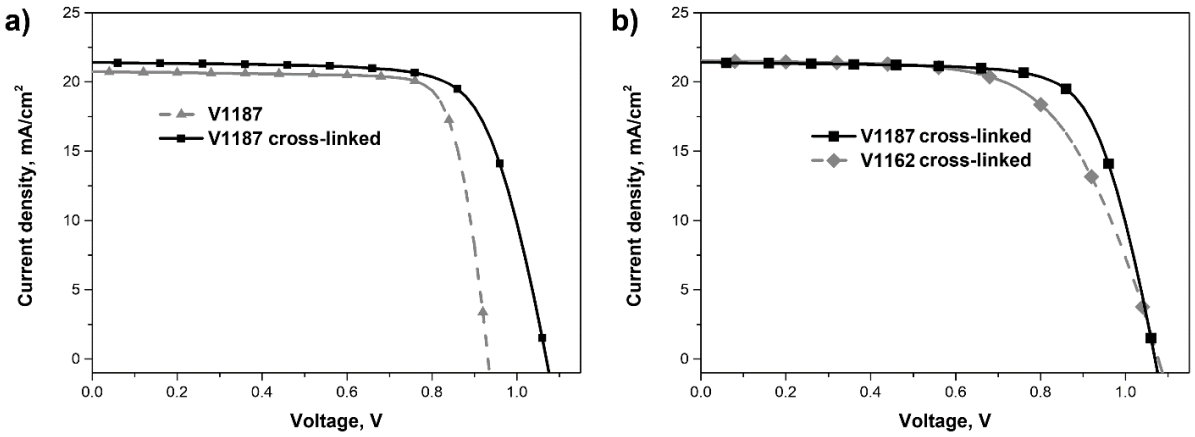

Figure 5. J/V measurements of the PSCs prepared with the new HTMs (reverse scan, from open to short circuit). a) comparison of the devices, prepared with the neat HTM vs cross-linked HTM; b) comparison of the performances of the two cross-linked HTMs.

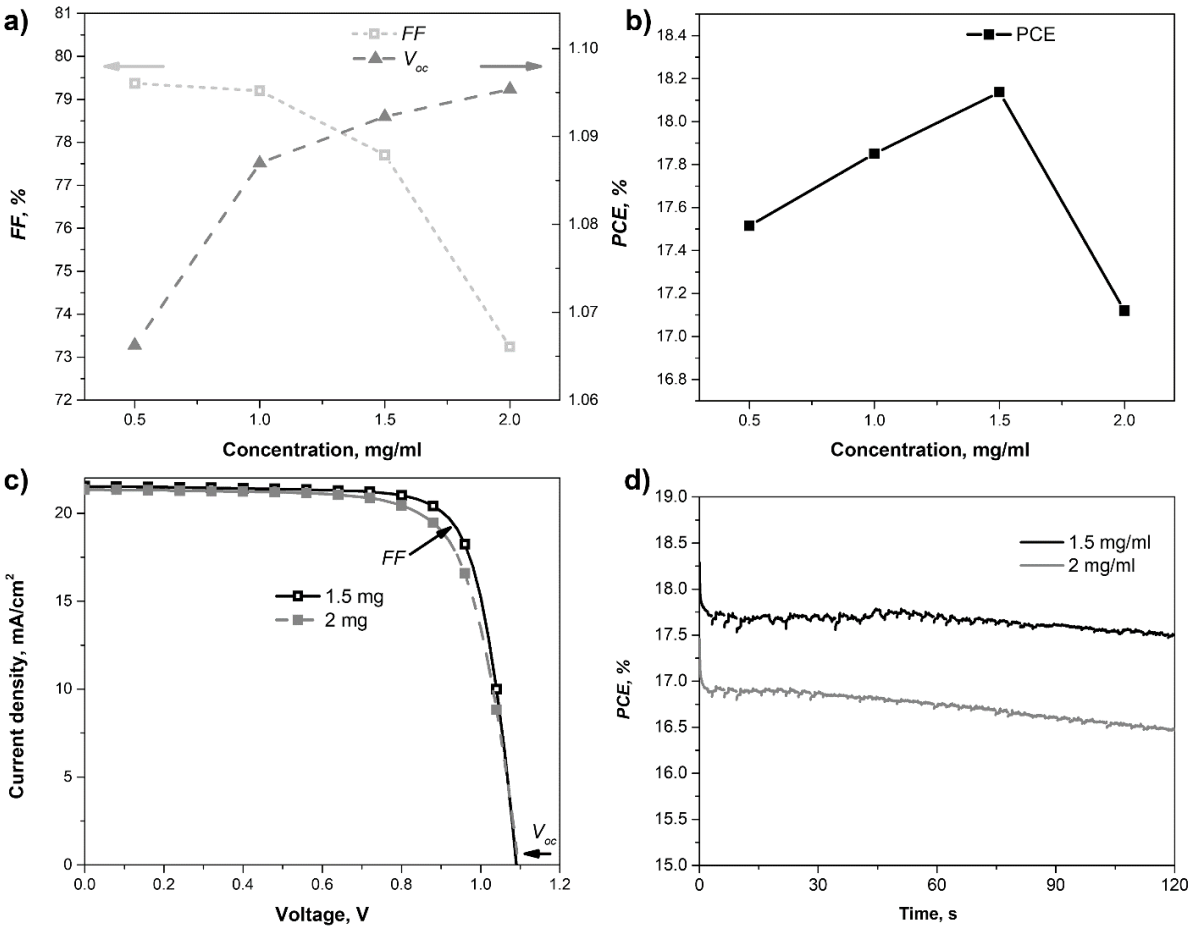

Figure 6. PSC analysis of cross-linked **V1187** films. a) Dependence of the *FF*, V_{oc}, and b) PCE on the concentration of the **V1187** solution. c) comparison of representative J/V characteristics (reverse scan, from open to short circuit) of **V1187**-based devices prepared from solutions with different concentrations and d) respective maximum power point tracking.

Table 1. Average performance parameters of the PSCs with new HTMs (prepared from 2 mg/ml in toluene). Data extracted from J/V scans, including the standard errors and the best performance parameters (in brackets). The statistics are based on 6–10 cells on different substrates.

Compound	J_{sc} (mA cm^{-2})	V_{oc} (V)	*FF* (%)	PCE (%)
V1162	21.19±0.12 (21.60)	0.846±0.013 (0.878)	75.8±0.2 (76.4)	13.60±0.25 (14.49)
V1162 cross-linked	21.55±0.14 (21.51)	1.036±0.014 (1.077)	61.7±0.8 (63.5)	13.78±0.35 (14.71)
V1187	21.34±0.16 (20.73)	0.891±0.020 (0.932)	79.3±0.4 (80.3)	15.08±0.35 (15.51)
V1187 cross-linked	21.95±0.15 (21.40)	1.040±0.012 (1.069)	71.1±1.8 (73.3)	16.21±0.35 (16.77)

Table 2. Average performance parameters of the PSCs with the **V1187** films, prepared from the solutions with the different concentrations. Data extracted from J/V scans, including the

standard errors and the best performance parameters (in brackets). The statistics are based on 6–10 cells on different substrates.

Compound	Concentration (mg/ml)	J_{sc} (mA cm^{-2})	V_{oc} (V)	*FF* (%)	PCE (%)
V1187 cross-linked	0.5	20.98±0.09 (21.18)	1.039±0.013 (1.066)	73.3±2.1 (79.4)	15.95±0.47 (17.51)
	1.0	21.42±0.12 (21.64)	1.057±0.014 (1.070)	72.7±3.4 (79.2)	16.48±0.88 (17.74)
	1.5	21.39±0.09 (21.61)	1.075±0.009 (1.092)	71.4±2.5 (77.7)	16.44±0.68 (18.14)
	2.0	21.31±0.10 (21.67)	1.077±0.007 (1.095)	69.2±1.2 (73.2)	15.88±0.33 (17.12)